NON IDEAL MOTION IN AIRBORNE SAR: ANALYSIS AND COMPENSATION

Manjula T R[1], Vasanth Kumar T R[2] and Shankar B B[3]

[1]*Department of ECE, Auden Technology and Management Academy, Bangalore-562 112.*
[2&3]*Department of ECE, Acharya Institute of Technology, Bangalore-560 090.*

Abstract

Motion compensation is an important part of SAR processing for high resolution air borne imaging sensors. The non ideal motion of the platform carrying radar, results in degraded image quality. This paper concerns the analysis and compensation of trajectory deviations in airborne Synthetic Aperture Radar (SAR) systems. Analysis of the received data spectrum is carried out with respect to the system geometry in the presence of linear, Quadratic sinusoidal and general aircraft displacements and presents an efficient new motion compensation algorithm. This method is verified with simulated SAR data.

1 Introduction:

Synthetic aperture radar (SAR) [1] is a remote sensing system used to obtain high resolution images of the observed scene. The device is mounted on on-board a platform (airplane, satellite or space shuttle) that, in the ideal case, moves with a constant velocity along a rectilinear trajectory. The scene is illuminated at constant time intervals and the received signal (raw data) contains information about its back scattering properties.

High geometric resolution in range (target to flight path distance) is obtained via transmission of linearly frequency modulated (chirp) pulses. On the other hand, high resolution in azimuth(flight direction) is the result of coherent data processing(focusing or pulse compression) [2] operation aimed at synthesizing an antenna array whose dimension is several times larger than the one of the real illuminating antenna mounted on board the platform

SAR raw data consists of a coherent superposition of the back scattered echoes from the imaged scenario. The backscattered echoes are modulated by the transmitted pulse(chirp pulse) and by the natural movement of the sensor. The image formation process consists of compressing the signal of each scatter, which is time dispersed(modulated) in the along track(azimuth) and cross track (range) direction

In airborne SAR systems deviations of the trajectory from the nominal one as well as attitude and forward velocity variations frequently occur mainly due to atmospheric turbulence. This introduce errors in the received raw data which degrade the quality of the SAR image .In particular, depending on magnitude and nature, motion error causes loss of resolution, decrease in image contrast, spurious targets, loss of geometric accuracy and reduction in signal to noise ratio.

To compensate for motion errors, flight information must be available at the raw data processing stage. Usually these are provided by inertial navigation units (INS) on board the aircraft. But the complexity, maintainability and reliability of INS units limit their application in motion compensation

Actual track

2 Translational errors

The translational errors refer to platform position displacements from a straight-line track. The translational motion geometry of the platform at zero Doppler [4] is shown in Fig. 1. These errors depend upon the range to each target and upon the reference height above the ground. Two primary errors arise from these deviations. First, a phase error is introduced to all targets. This disrupts target phase histories and leads to image defocusing and shifting. Second, if the translational errors are large enough, they can cause target responses to drift into neighboring range bins.
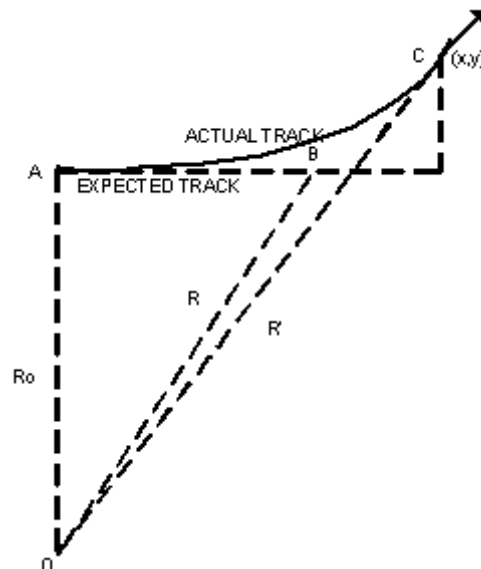

Fig. 1: A comparison of the path length for expected and actual tracks

An object 'O' is imaged by sensor traveling along actual track 'AC' from origin A $(0,0)$ to position $c(x, y)$ at range distance $R^{'}$ with $R0$ being broadside Range. The expected track is

'AB' for which the object is imaged at range distance R . i.e., the object is sensed at range R when it is traveling at in straight line path, and at range R' when it deviates from ideal track The range difference (error) is given by the difference between the expected and actual range $\Delta R = R - R'$. The corresponding phase error is $\Delta\varphi = \dfrac{4\pi}{\lambda}\Delta R$
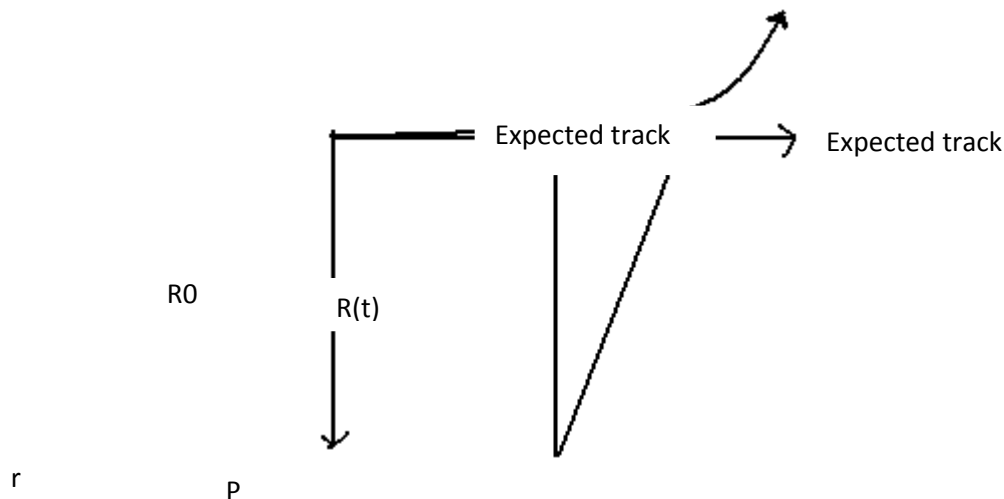

Fig. 2: A comparison of the path length for expected and actual tracks

From the above figure the difference between the expected and actual range 'ΔR' is approximated as displacements in x, r direction

The displacement in 'x' direction, $x = (v + \Delta v)t + \dfrac{a_x t^2}{2}$

The displacement in ' r ' (LOS) direction, $r = v_\gamma t + \dfrac{a_r t^2}{2}$

Where, $v \,\&\, v_r$ are along track and radial velocity respectively, $a \,\&\, a_r$ are corresponding acceleration, ΔV is along track velocity mismatch.

The range error which is difference between actual ranges $R(t)$ & expected R_0 is given by

$$\Delta\phi(t) = -\frac{4\pi}{\lambda}\Delta R(t)$$

The associated phase difference (error) is

$$\cong -\frac{4\pi}{\lambda}\left[V_r t + t^2\left(\frac{V^2}{2R_0} + \frac{a_r}{2} + \frac{V^2}{R_0}\cdot\frac{\Delta V}{V}\right) + \ldots\ldots\right]$$

$$\equiv \alpha t - (\beta + \Delta\beta(t))t_2$$

Where α is known as Doppler centroid [4] parameter given by equation $\alpha = \dfrac{4\pi V_r}{\lambda}$

β and $\Delta\beta$ are focus parameters given by equation $\beta = \dfrac{2\pi V^2}{R_0 \lambda}$ and

$$\Delta\beta = -\frac{4\pi}{\lambda}\left(\frac{a_r}{2} + \frac{V^2}{R_0}\cdot\frac{\Delta V}{V}\right)$$

α is a linear phase term. The effect of the linear phase to the point target is to cause an azimuth shift but make no change to the waveform. That is, linear phase error has no impact on SAR image focus, but shifts response in azimuth. From above formulation, V_r is the key factor of Doppler centroid parameter, so the image will shift at azimuth when V_r is not zero; the variation of V_r makes the distortion in the resultant image.

$\beta + \Delta\beta$ is the second phase error term, which can widen the main beam of the target response, leads to higher sidelobes, cause a loss in magnitude and resolution. It means defocus. The typical defocus and distortion are caused by slant range, and along-track uncertainties. These depend on fluctuation in the focus parameter $\Delta\beta / \beta$, which is due to mismatch between nominal and actual along track velocities $\Delta V / V$, or due to existence of across track acceleration a_r component. The above analysis is evaluated and the simulation results are presented in section

Motion Induced Phase Errors on the Image

Phase error category	Image Effects
Low frequency errors	Geometric distortion; loss of resolution
High frequency sinusoidal phase errors	Loss of contrast; spurious targets

Low frequency motion errors: Are those position errors with variations period lesser than azimuth aperture time, and low frequency errors encompass linear, quadratic phase errors (QPEs) and higher order phase errors.

Linear phase error: By definition the phase of the linear phase error varies linearly with position along the data space. Sources of low frequency phase errors include velocity and acceleration errors, variations in the velocity of the radar along flight path, give rise to linear phase error [5] and results in the shift of the point target response in azimuth direction

Quadratic phase error (QPE): Varies quadratically with position across the data space. QPE causes broadening of the image processing system's impulse response width. This broadening causes an effective decrease in image resolution and tends to smear targets. However, the effect

of QPE is not limited to the main lobe, one of its first effects is to fill in side lobe nulls and increase integrated side lobe ratio ISLR

Acceleration error term causes a quadratic phase error, which results in maximum deterioration of the image. If the quadratic coefficient is space invariant, the effect is uniform defocus over the scene. Quadratic phase error broadens the main lobe of the target impulse response and thus degrades the resolution of the image

High frequency motion errors: Are those position errors with periods larger than or equal to azimuth aperture time. High frequency errors include sinusoidal and random phase errors. High frequency phase errors with more rapid variations of period larger than the coherent aperture interval over the processing aperture are referred to as sinusoidal phase error. The phase term representing a sinusoidal phase error across the aperture has the form $e^{j\phi_0 \sin(2\pi f_e t)}$

A sinusoidal phase error causes paired echoes to appear in the system impulse response. This effect means high peak side lobes are present, which may be interpreted erroneously as separate targets when in fact, they are spurious targets. The primary effect of high frequency random phase errors is to take main lobe energy and distribute it over several sidelobes leading to poor image contrast

Motion Error Compensation (Moco) for spotlight Synthetic Aperture Radar

The received signal is modeled on translational errors by introducing fluctuations in range by variations in the speed of radar along the flight path.

Demodulated SAR signal [4] given by exponential equation

$$S_0(\tau, n) = e^{\left(\frac{-j4\pi \ f_c R(\eta)}{c}\right)} e^{\left(j\pi \ k_r \left(\frac{\tau - 2R(\eta)}{c}\right)^2\right)}$$

(1)

η is the (along track) azimuth time , τ is the range (fast) time , c is the speed of light, k_r is the chirp rate , f_c is the center frequency and $R(\eta)$ is slant range and is function of azimuth time η

With translational motion error, expected range $R(\eta)$, becomes aberrated range $\Delta R(\eta)$

The approach of motion compensation is to split the deviation errors into

➢ Range independent errors
➢ Range dependent errors

$$\Delta R(\eta) = \Delta R_{ref}(\eta) + \Delta R_{diff}(\eta)$$

Where ΔR is the total displacement range error, ΔR_{ref} is the Range independent errors ΔR_{diff} is the Range dependent error

This changes the demodulated signal Eq. (1) to

$$S_m(\tau,n) = e^{\left(\frac{-j4\pi f_c R(\eta) + \Delta R_{ref}(\eta) + \Delta R_{diff}(\eta)}{c}\right)} . e^{\left(j\pi k_r \left(\frac{\tau - 2R(\eta) + \Delta R_{ref}(\eta) + \Delta R_{diff}(\eta)}{c}\right)^2\right)}$$

ge independent errors are those whose magnitude of deviation is small compared to the synthetic aperture length and the displacement errors is same for all the targets within the scene and is equal to the one at the scene center.

Moco is implemented as 2 stage compensation [4] referred to as

➢ *First order Moco* and
➢ *Second order Moco*

First order Moco applies phase correction to range independent errors and provides bulk error compensation. It is performed directly on the raw data.

Second order Moco corrects range dependent errors, and is applied to the range compressed data.

SAR Motion Compensation Processing Algorithm

For range independent errors, the displacement error for all targets within the beam equal the one of the center beam. Based on this, Range independent errors are extracted with respect to a reference range 'R_0' (usually chosen to be the scene center)

$$\Delta R_{ref} = R_1 - R_0$$

Where R_1 is the actual range measured, ΔR_{ref} is the range independent error, R_0 is the range to the scene center (broadside range)

Since Range independent errors are independent of slant range variation, the bulk Moco is performed as a preprocessing step on the raw data by a phase multiplication [6],which is obtained by expanding Eq. (2) and selecting range independent error terms , is given by

$$M_1 = e^{\left(\frac{-j4\pi\Delta R_{ref}(\eta)\left(-f_c c - k_r \tau c + k_r \Delta R_{ref}\right)}{c} \right)^2}$$

Where f_c the carrier frequency is k_r is the chirp rate and c is the speed of light.

This correction, while not completely correct the phase errors, puts the data in approximately the correct location, reposition the raw data in the azimuth direction while canceling any azimuth shift.

The data is then range compressed and second order Moco is applied after transforming the range compressed SAR data to the signal domain.

Second order Moco addresses displacement errors which are range dependent. The residual error which remains after performing first order Moco is range dependent, which takes into account the variations in the path length (Range).Due to these variations, range bins are drifted from their positions leading to azimuth defocusing which arises due to mismatch between azimuth chirp and the matched filtering reference function. Range dependent errors are extracted as a range bin drift for each received pulse and for all range bins over Synthetic aperture length and compensated for by a phase multiplication with range compressed data

Phase correction is given by

$$M_2 = e^{-j8\pi k_r \Delta R_{ref}(\eta)\left(\frac{\left(\Delta R_{diff}(\eta)+R(\eta)\right)}{c^2}\right)}$$

$$\cdot e^{\left(j4\pi k_r \frac{\Delta R_{diff}(\eta)^2}{c^2} - j\frac{j8\pi k_r R(\eta)\Delta R_{diff}(\eta)}{c}\right)}$$

$$\cdot e^{\left(j4\pi f_c \frac{\Delta R_{diff}(\eta)}{c}\right)} \cdot e^{\left(j4\pi k_r \tau \frac{\Delta R_{diff}(\eta)}{c}\right)}$$

where $\tau = 2R/c$
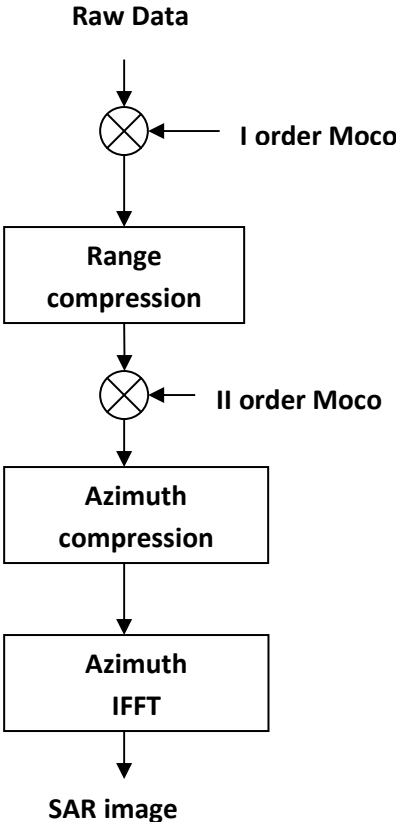
Fig. 3: Motion compensation algorithm

Results

SAR data simulated with parameters described below is used to verify the proposed motion compensation algorithm

Pulse width	3×10^{-06} secs
Cross range resolution	3m
Range resolution	3m
Speed of the radar platform	100 m/s
Range	10000m
Pulse repetition frequency	500 Hz
Carrier frequency	6×10^{06} Hz
Azimuth swath width	100m
Range swath width	100m
Synthetic aperture length	32.5m

To evaluate the performance of the motion compensation algorithm, for translational errors, single point target is considered at the scene center to generate data. The received data is preprocessed and applied to Moco algorithm. The evaluation is performed in the view of considering real conditions; the received signal is modeled on translational errors by introducing fluctuations in range by variations in the speed of radar along flight path.

Figure.4.1 illustrates, with the introduction of linear phase error in the form of velocity variations along the flight path results in shift of the target response in azimuth direction

Figure.4.2 illustrates, the QPE results in broadening of the main lobe leading to loss of contrast

Figure.4.3 illustrates Sinusoidal phase errors causes paired echoes to appear in the impulse response of the target. This effect means, high sidelobes are present which may be interpreted erroneously as separate targets, when infact they are spurious targets. Moreover small targets are masked by adjacent strong side lobes. The higher the amplitude of the sinusoidal displacement, the larger the number of significant replicas (echoes).

Applying I and II order motion compensation results in impulse response as shown in **Figure.5** Range independent errors are corrected in first level of Moco as a result of which data is repositioned in the azimuth direction canceling any azimuth shift. While the range dependent errors which are responsible for mian lobe broadening are corrected in second level of Moco

Figure. 6 illustrates an aberrated image of 3 point targets with the introduction of high frequency sinusoidal and random motion error with amplitude of 3m .

Figure.7 shows 3 point target image, after motion compensation

Conclusion

A detailed analysis of the motion errors in Synthetic aperture radar, their effect on the impulse response of the target is discussed. Analysis of the received data spectrum is carried out in the presence of linear, quadratic and sinusoidal displacements. Results shows that motion errors lead to image defocus, azimuth shift and produce spectral replicas which strongly impair the quality of the focused image. An improved motion compensation algorithm for SAR has been proposed , implemented and evaluated.Final results on simulated data aimed at validating the whole analysis and proposed procedure are presented. The results show that it properly corrects the effects of non ideal motion.The proposed method can be implemented in place of the traditional method to improve processing efficiency and accuracy

Fig.4.1: Linear phase error
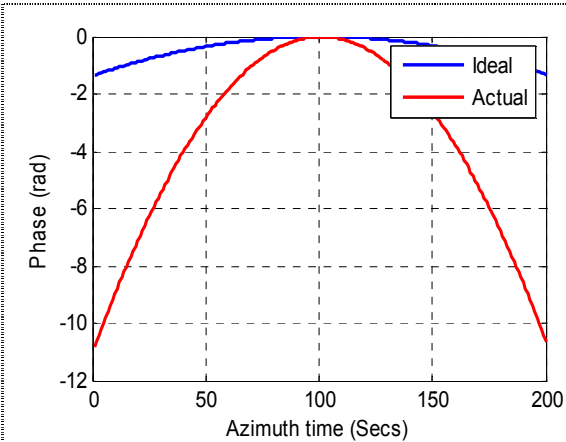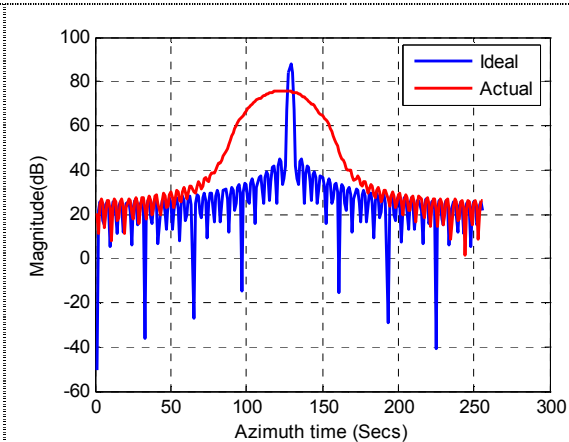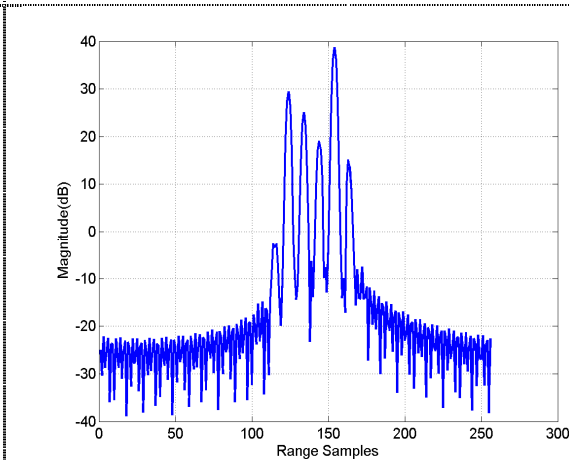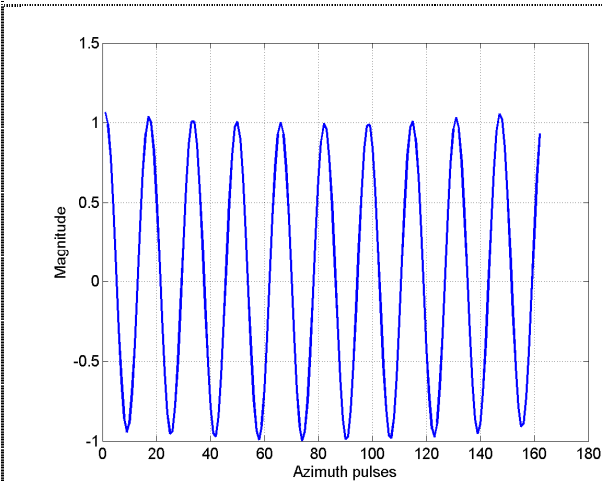

Azimuth shift due to linear phase error
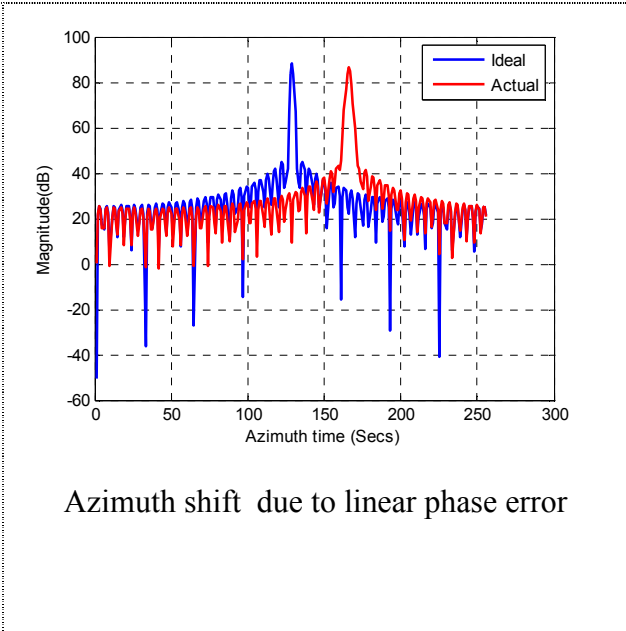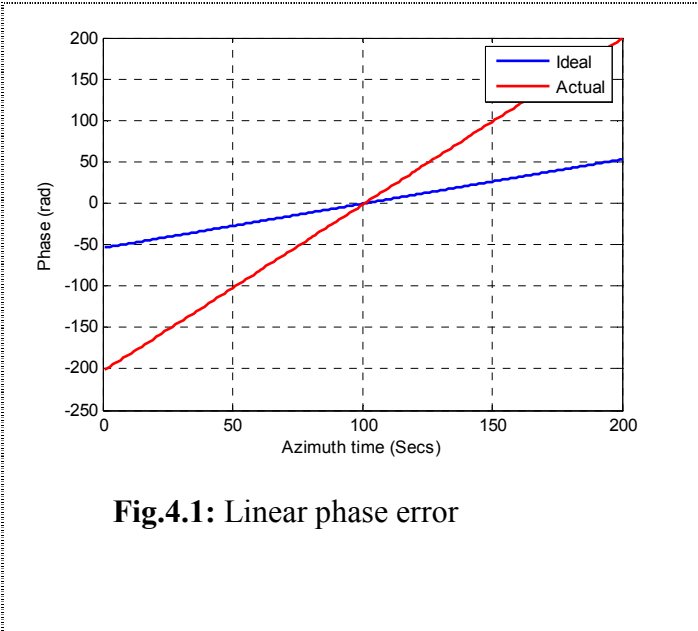
Fig. 4.2 Quadratic phase error(QPE)

Broadening of the main lobe due to (QPE)

High sidelobes due to high frequency errors

| **Fig. 4.3** High frequency errors | |

Target response after first level of Moco

Target response after second level Moco
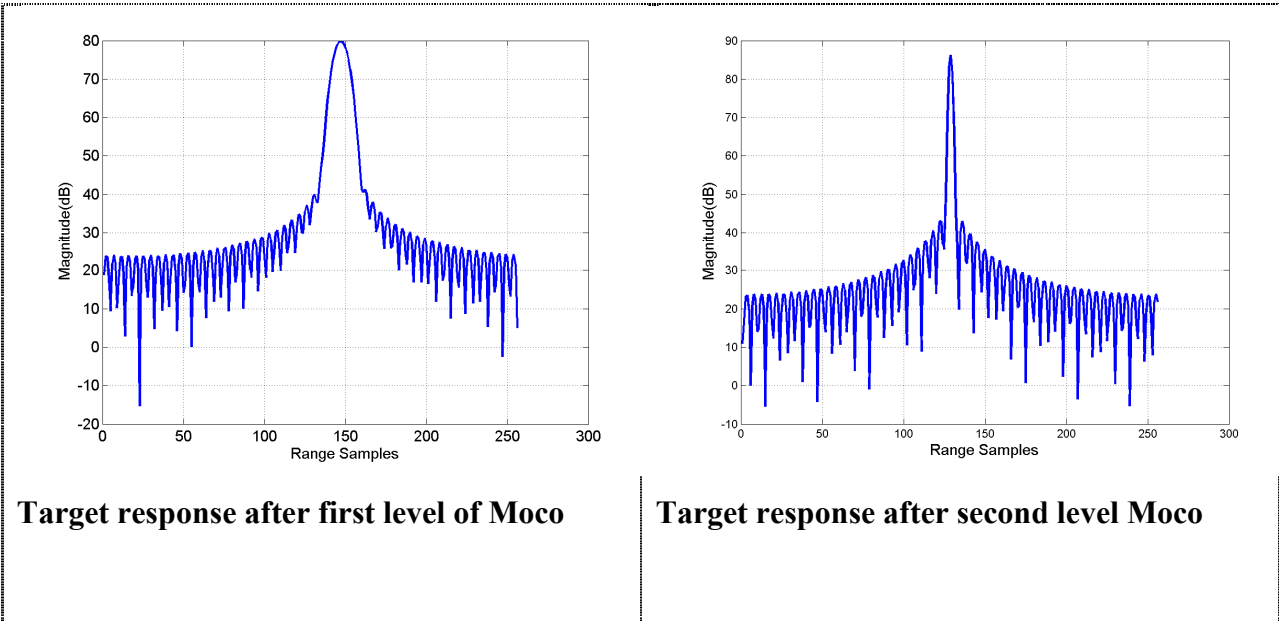
Fig. 5: First and second order motion compensation

Range compressed image (with error)   **Azimuth compressed image(with error)**
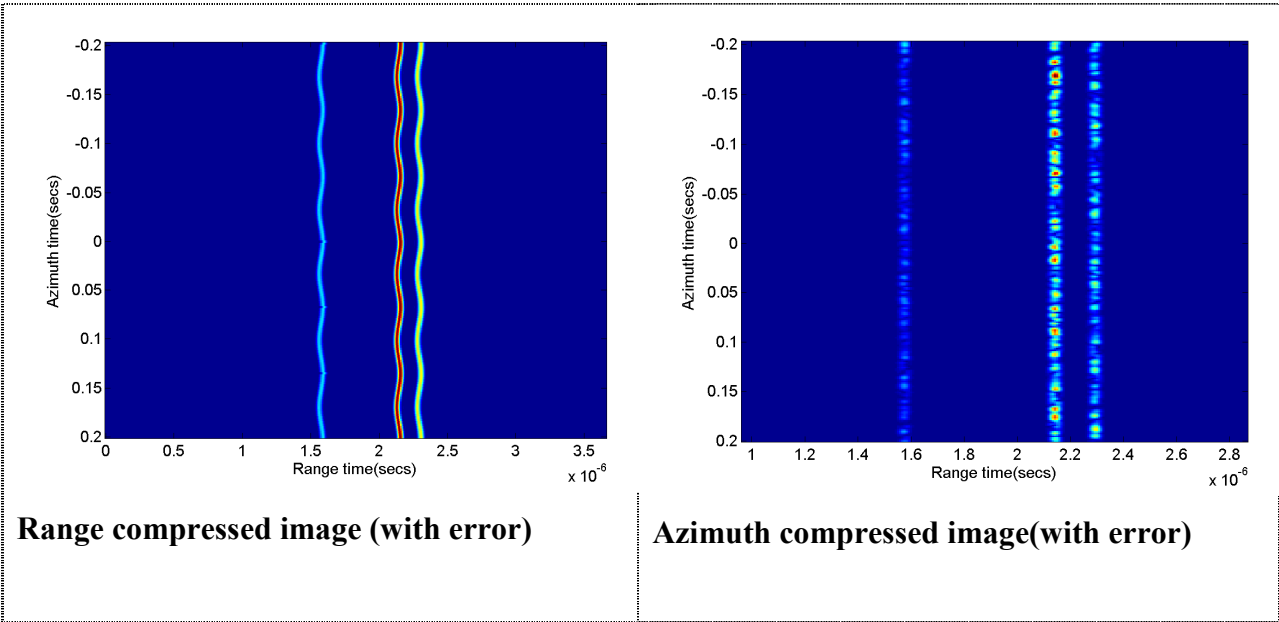
Fig. 6: Range and azimuth compressed image with motion errors

Range Compressed Image after First Level Moco

Azimuth Compressed Image after Second Level of Moco
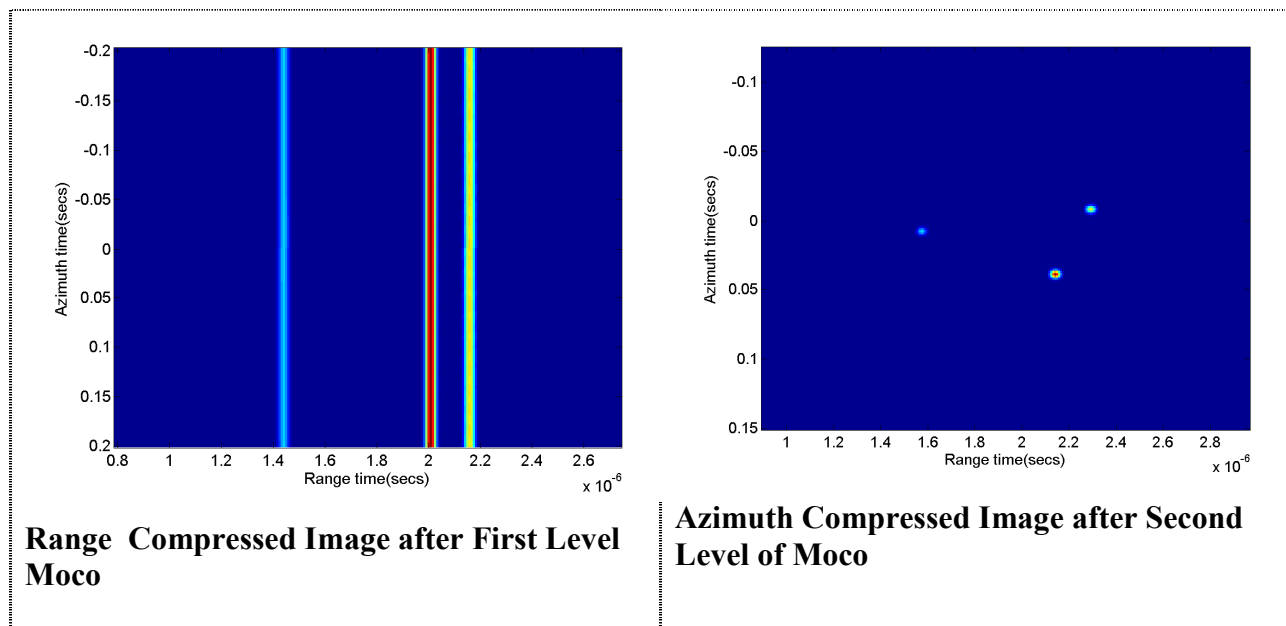
Fig. 7: First and second order motion compensation of 3 point image

References:

[1] George W. Stimson Scitech, *Introduction to airborne radar* Publishing Inc..

[2] Bassem.R.Mahafza, *Radar Systems and analysis design using MATLAB*

[3] Giorgio Franceschetti, Riccardo Lanari, *Synthetic Aperture Radar Processing*, CRC Press, New York, 1999.

[4] I.G. Cumming, F.H. Wong, *Digital Processing of Synthetic Aperture Radar Data*, Artech House, 2005.

[5] Walter G. Carerra Ron, S. Goodman Ronald M. Majewski, *Spotlight Synthetic Aperture Radar Signal Processing Algorithms* 1995 Artech House

[6] Evan.C. Zaugg, David.G Long, *Improved SAR motion compensation without interpolation*

[7] John C. Kirk, Motion, *Compensation for Synthetic Aperture Radar*. IEEE transactions on AES May 1975

[8] Henry D. Baird, Jr, *Motion compensation for synthetic aperture radar and its compatability with strap down inertial Navigation sensors on highly maneuverable aircraft, 1985*

[9] P.A. Rosen, S. Hensley, K. Wheeler, G. Sadowy, T. Miller, S. Shaffer, R. Muellerschoen, C. Jones, H. Zebker, S. Madsen, *A New NASA Airborne SAR System for Science and Technology Research*, 2006 IEEE Radar Conf., pp. 24-27, April 2006.

[10] E.C. Zaugg, D.L. Hudson, D.G. Long, *A Small, Student-Built SAR for UAV Operation*, Proc. Int. Geosci. Rem. Sen. Symp. Denver Colorado, pp.411-414, Aug. 2006.

[11] Madsen S.N, *Motion Compensation for Ultra Wide Band SAR* Proc. Int. Geosci. Rem. Sen. Symp., Sydney, NSW, pp.1436-1438, July 2001 .

[12] A. Meta, J.F.M. Lorga, J.J.M. de Wit, P. Hoogeboom, *Motion compensation for a high resolution Ka-band airborne FM-CW SAR*, EURAD 2005, pp. 391-394, Oct. 2005.

[13] E.C. Zaugg, D.G. Long, *Full Motion Compensation for LFM-CW Synthetic Aperture Radar*, Proc. Int. Geosci. Rem. Sen. Symp., Barcelona, Spain, Jul. 2007.

[14] A. Moreira, Y. Huang, *Airborne SAR processing of highly squinted data using a chirp scaling approach with integrated motion compensation*, TGRS, vol. 32, pp. 1029-1040, Sept. 1994.